Development of a Method to Derive Design Guidelines for Production-suitable Support Structures in Metal Laser Powder Bed Fusion

S. Lammers[*,†], T. Lieneke[*,†], D. Zimmer[*,†]

*Chair of Design and Drive Technology, Paderborn University, 33098 Paderborn, Germany
†Direct Manufacturing Research Center (DMRC), Paderborn University, 33098 Paderborn, Germany

Abstract

Solid support structures in metal laser powder bed fusion have a significant influence on the economic applicability, component quality and process stability and represent a central challenge for widespread industrial use. As the connection of the components to the building platform by supports is essential, the negative effects must be minimized at the same time as the supporting effect is optimized. Within the scope of this study, a standardized method is developed that allows the investigation of several support structures and parameters with regard to their influence on the target variables: component quality, process efficiency and stability. In addition to the proof of general suitability, the applicability is investigated using so-called standard elements. Based on the experimental results, design guidelines are derived, which will serve as a basis for decision-making during the selection of support structure for an individual application.

Introduction

In contrast to conventional, subtractive manufacturing processes, additive manufacturing involves building up components element by element or layer by layer, without tools. [1]. The layer-by-layer build up is based on the underlying three-dimensional CAD model, which is converted into a sequence of two-dimensional layer models [2].

The simplification of the three-dimensional problem into many two-dimensional layers induces design freedom. In this way, structures can be realized that would be difficult or impossible to produce using conventional manufacturing processes [3]. In addition to complex external free-form surfaces, internal structures such as cooling channels close to the contour, structure-optimizing grid fillings or force-flow-optimized sandwich structures can also be utilized using additive manufacturing processes [4]. The manufacturing of topology-optimized or bionic structures is also possible [5, 6]. These advantages result in a large lightweight design potential and consequently a large potential for material-efficient production as well as resource-saving operation of additively manufactured components. In addition, function integration can reduce the number of components required to fulfill different functions and reduce the assembly effort, which enables cost reduction and further weight reduction. [7, 8, 9, 10]. The Metal Laser Powder Bed Fusion (LPBF) process, among others, is established for the additive manufacturing of metallic components.

However, LPBF implicates process-specific restrictions and disadvantages. For example, the process is characterized by a high proportion of manual, time-intensive work steps. In addition to the support structure generation and data preparation, which take place before production, these also include downstream processes such as cooling, separation from the building platform, powder removal and support structure removal. The support structure-related steps are particularly inefficient, but unavoidable, because support structures are needed in the LPBF process for a robust build process, to minimize warpage, to fix the components during the process, and to dissipate the process-induced heat. After the build process, however, these support structures are largely unwanted and must be removed at great expense. Since they also increase material requirements and production times, they are considered as a necessary evil. Other post-processing methods such as heat treatment, machining or surface finishing may also be necessary to improve dimensional accuracies, surface qualities, porosity and mechanical properties inherent to the process. Compared to conventional processes, the low production speed for large series is also a limiting factor. In addition, the component size is limited by the available build chamber of the additive manufacturing system [3; 11]. It is unknown, how long these

disadvantages will remain. However, the highly dynamic market in the field of additive manufacturing and extensive research projects give reason to hope for significant improvements [12, 13, 14, 15].

Motivation

In order to minimize or completely eliminate the inherent disadvantages of the LPBF process and the support structures, profound fundamental knowledge is required. To this end, design guidelines for users have been developed in recent years, which provide support for the production suitable design of components for additive manufacturing [4, 12, 16, 17, 18] or assistance for the finishing suitable design of additive components [13, 15, 19]. Design guidelines with respect to optimized support structure generation are also partially available [14, 20, 21, 22]. However, these often only deal with the variation of a support structure parameters and its influence on the component properties or on the process.
This paper therefore focuses on the development of a standardized method for the quality assessment of support structures with respect to different component and process properties under variation of support structure parameters. The method should enable the user to determine the influence of different support structure parameters, such as hatching, tooth geometry or fragmentation, on the component or the process. As a result, it should be possible to derive design guidelines for successful support structure design and to benchmark different support structures. These design guidelines with reference to support structures are to be called production-suitable support structure design guidelines in the following.

Support structure parameters

The most common support structure in use is the block support shown in Figure 1. It is a support structure composed of narrow walls of wall thickness b_W in a rectangular grid pattern. The block support is used to support voluminous and massive components as well as for smaller components [14]. The center-to-center spacing a_H of adjacent support walls in the rectangular grid is called the hatch distance.
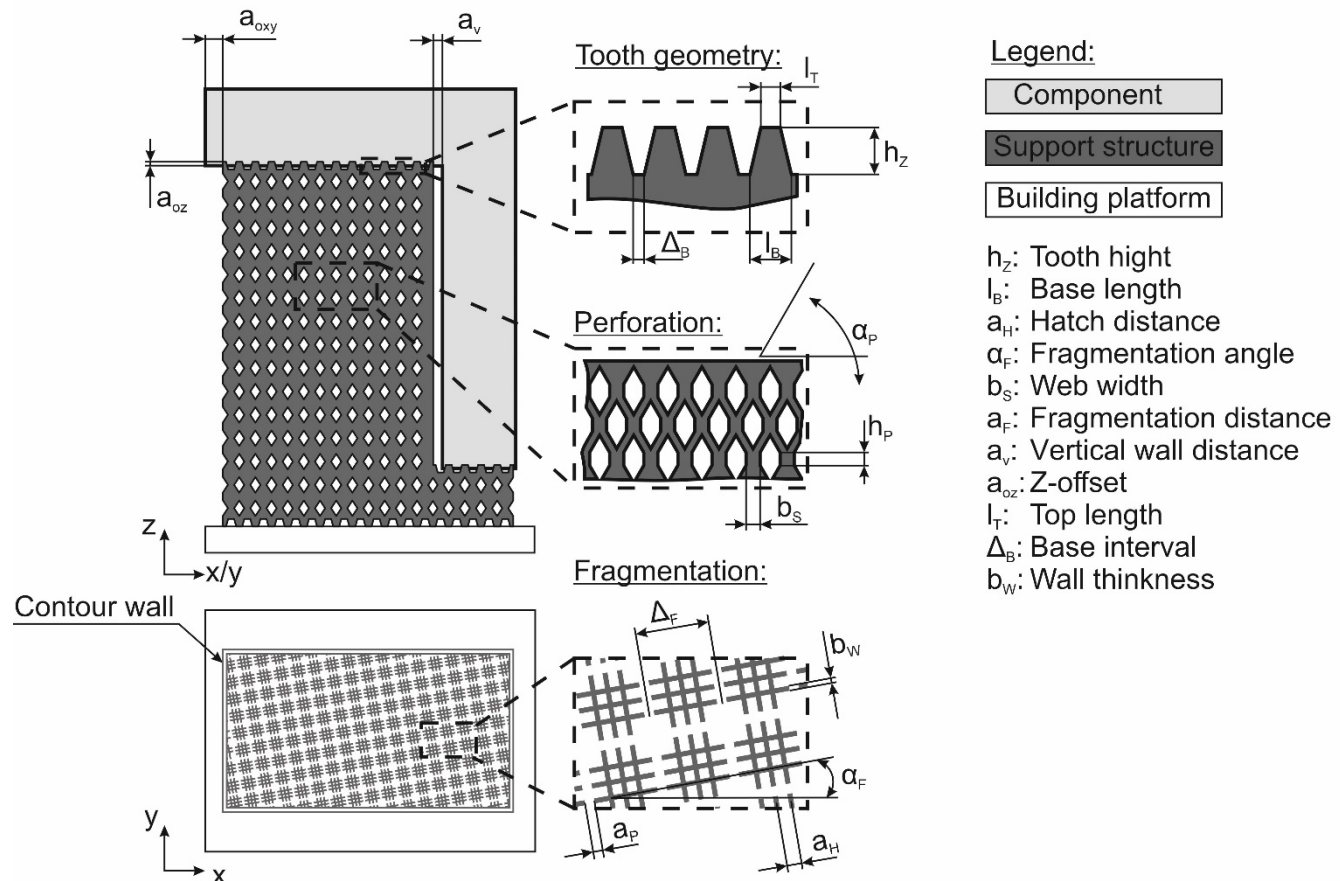

Figure 1: Relevant block support parameters. At the top the side view with perforated side of contour walls. At the bottom the top view on the support structure fragmentation.

The contact area to the component and the build platform is usually designed with so-called teeth. The tooth geometry is described by the support structure parameters top length l_T and tooth height h_Z. Fragmentation is another support structure parameter. It divides the lattice scheme in the xy-plane into adaptable segments. Perforations, on the other hand, introduce interruptions in the support structure walls in the z-direction. The objective in the support structure parameter selection is to design a support structure that has sufficient resistance to residual stresses and process forces, while allowing better peelability and powder removability. The parameters hatch distance a_H, wall thickness b_W, top length l_T and the tooth height h_Z mentioned here have the greatest influence on these properties and will be used for the further investigations [8, 23].

Method to derive design guidelines for production-suitable support structures

The standardized procedure of the method to derive design guidelines for production-suitable support structures is described in the following. It is intended to enable a comparison of different variants of support structures with regard to criteria of component quality, process efficiency and stability. In addition, the usefulness in practical applications, such as inclined overhangs or internal contours, will be examined more in detail. The method is divided into the five steps shown in Figure 2.
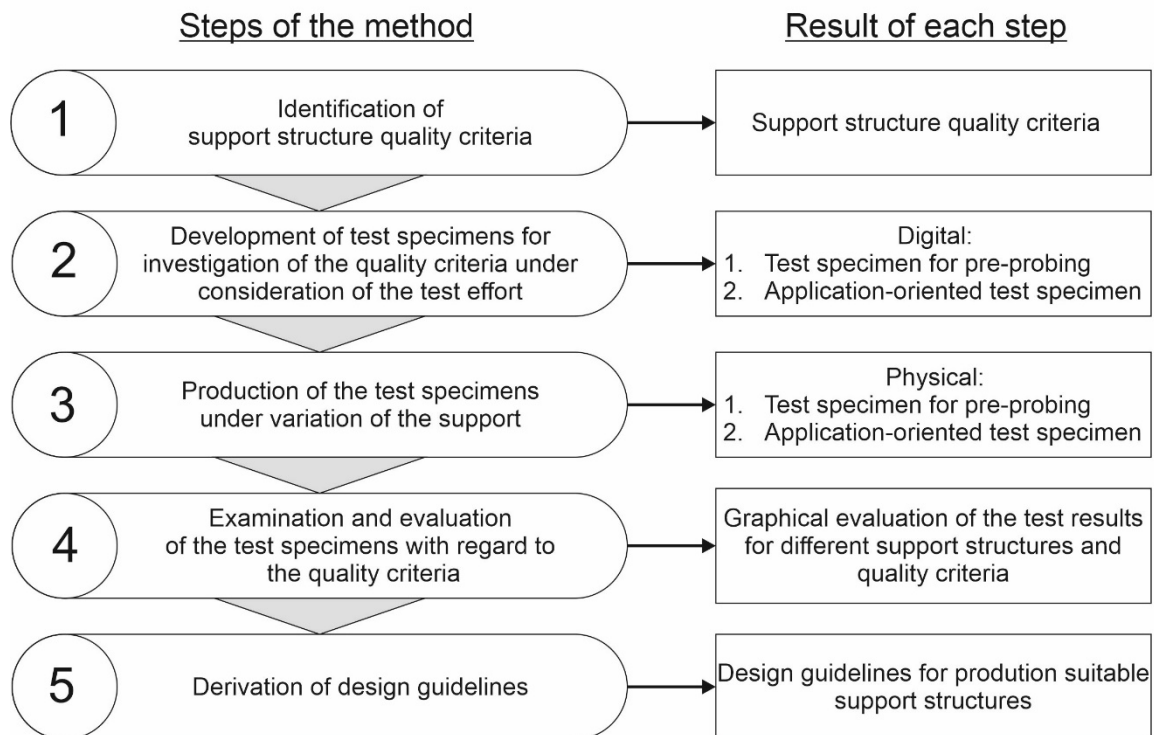

Figure 2: Schematic structure of the method to derive design guidelines for production-suitable support structures.

The first step is to identify relevant quality criteria for support structures that influence component quality, process efficiency and stability. These criteria must be determined for different support structures in order to be able to perform a quality assessment. In a second step, test specimens will be developed which can be supported by different support structures and allow the investigation of relevant quality criteria. In order to keep the test effort low, small, material-saving test specimens were developed for pre-probing, which allow an efficient investigation of a large number of different support structures in a few build jobs. In order to evaluate geometries that are closer to the application, further test specimens were developed. These are based on standard elements already used in ADAM [16]. These so-called application-oriented test specimens are limited to support structures for whom a basic suitability could be demonstrated during the pre-probing. The test specimens are dimensioned in such a way that they can be manufactured on common equipment with a building platform size of at least 250 x 250 mm. In the third step, the two test specimen types are manufactured

using the LPBF process. In the fourth step, the test specimens are examined with regard to the quality criteria for support structures identified in step 1. The test results are entered in a clear graphical evaluation, which shows the effect and interaction of different support structure parameters on the quality criteria. In the final step, design guidelines are derived based on the results to provide designers with basial rules for application-adapted support structure design. The method is structured to be able to integrate further boundary conditions such as production systems, materials, production parameter sets or support structure parameters.

Step 1: Identification of support structure quality criteria

The quality criteria were selected on the basis of previous investigations and the documented experience of the AM community in the form of scientific publications and field reports. They are marked in a bold font in this chapter.

As a basic quality criterion, a visual inspection of the **imaging accuracy** is first performed. The actual geometry is compared with the target geometry. Any conspicuous features, such as fractures, powder deposits or deformations, are recorded.

In the investigation of the attainable component quality, the measurement of the shape and dimensional accuracy of the test specimen is carried out in all three spatial directions. For the dimensional stability in the z-direction, the maximum distortion at the bottom of the test specimen is determined. If the deformation in the positive z-direction in the area of the uppermost layer exceeds the value of the layer thickness during the process, the process can be aborted due to the collision of the recoater with component areas [22]. It is known that the risk of collision of the recoater comes from the deformation at the current top of the component. However, the strongest deformation in the z-direction is present at the bottom side of the components. If this deformation is subcritical, the shape deviation is usually compensated by the further coating and exposure process and thus no longer occurs on the top side of the finished component. For this reason, the measurement of dimensional accuracy in the z-direction is limited to the bottom side of the test specimen. By determining the **dimensional accuracy in the z-direction**, a possible sagging of the lowest test specimen layer in the further course of the process is detected. Preliminary investigations have shown that successive shrinkage in the z-direction can be observed in some support structures. This results in a positive dimensional deviation in the z height of the component and a negative dimensional deviation at the support structures, as the contact area between the support structure and the test specimen shifts in the negative z direction, while compensation takes place on the upper side due to the continuous coating. Another reason for a dimensional deviation in the z-direction can be a sinking of the melt into the powder bed or the undesired sintering of powder particles on the underside of the component [8].

When measuring the **shape and dimensional accuracy in the xy-plane**, deviations in the test specimen width and depth are to be investigated. As the layers cool, the material contracts, causing tensile residual stresses in the top layer and induced compressive residual stresses in the layers below. This can induce dimensional deviations of the component width and worsen or prevent the connection to the support structures. Furthermore, the machining of the components to revise the dimensional deviations reduces the process efficiency [22].

In addition to shape and dimensional accuracy, **surface roughness** influences component quality. The measurement of surface roughness is limited to the underside of the test specimen, since this represents the contact surface to the support structure. Negative effects on the surface quality are to be expected from remaining support residues as well as from adhering and not completely melted powder particles [21]. In addition to the negative influence on the component quality, a pronounced surface roughness often necessitates further post processing, especially in the area of fits and functional surfaces, which reduces the process efficiency [4, 8, 9].

When designing support structures, a compromise must be found between sufficient strength and the **removability of support structures** [7]. For the industrial use of LPBF, the process efficiency must be increased by reducing the manual post-processing effort. In this context, simplified removability of the support structures is of particular importance [3, 23].

In the case of software-supported automatic support structure generation (e.g. via Materialise Magics), in which adjustments of individual parameters may have to be made, the **data preparation time** varies

depending on the number of necessary settings. If the support structures are even created completely manually or a unit cell is designed for cellular supports, a significantly greater time requirement can be assumed. In addition to the data preparation time, the necessary **data volume** is also recorded. For example, a massive increase in storage capacity can be expected for very complex, filigree support structures with large surfaces. This poses challenges for the data infrastructure. In addition, delays in the process chain are to be expected due to an increased time requirement for slicing the build job and loading it on the LPBF system.

Material consumption also determines the efficiency of the process. This is often opposed to the requirement for sufficient mechanical resistance of the support structures [22]. Both the material consumption of the support structures and the amount of powder which are enclosed by the support structures and cannot be removed via spaces between the teeth, perforations or fragmentations must be taken into account. This residual powder poses a risk of contamination and may not be reusable due to contamination or oxidation [5].

Step 2: Development of test specimens for the investigation of the quality criteria under consideration of the test effort

Two different test specimen geometries are used to pre-test a large number of different parameter combinations for support structures. These are referred to as PK1.1 and PK1.2 in the following. The basic support structure quality criteria defined in step 1 can be investigated with these. A small number of test specimens with reduced material consumption is desirable without reducing the significance or reproducibility of the results.

PK1.1 is a simple cuboid basic geometry, which is shown in Figure 3. The simple test specimen geometry is intended to minimize any influence of the test specimen geometry on the effects of the support structures. Furthermore, the small test specimen dimensions are suitable for manufacturing as many test specimens as possible in one build job. Thus, 81 parameter combinations can be investigated with one build job on widely used machines with a minimum build platform size of 250 x 250 mm, which corresponds to a full factorial test plan with four factors of three factor levels each. This experiment can be easily and meaningfully extended. In addition, the expected distortion usually starts from the corners, since these are particularly exposed areas, as the surrounding powder makes heat dissipation difficult [24]. Overall, despite its small dimensions, the square base is a geometry that is particularly susceptible to distortion and on which meaningful results can be expected for the various combinations of support structure parameters.

Below the test specimen, the examined support is inserted with a height of 4 mm, which corresponds to a widely used minimum support structure height. For the measurements on the test specimens, a clamping in form of an 8 mm x 8 mm cuboid was manufactured, the influence of this cuboid on the quality criteria can be precluded because of its subsequent production during the build job.

After the production of PK1.1, a measurement of the shape and dimensional accuracy in the xy-plane and the positional accuracy of the test specimen top in the z-direction on the building board is carried out. This is followed by an assessment of the removability of the support structures. After the support structure has been removed, the test specimens are examined for the dimensional accuracy of the bottom, since the highest distortion can be assumed on there. In addition, the dimensional accuracy in z-direction can be determined. Subsequently, the surface roughness of the bottom of the test specimen is measured in order to investigate the influence of the support structure residues and the fracture surfaces. Furthermore, the time required for data preparation and the resulting data volume can be determined for the test specimens PK1.1.

The PK2.1 test specimen, also shown in Figure 3, is used to investigate material consumption. Its basic geometry was used by GRALOW ET AL. for corresponding tests and has proven to be suitable [20]. Due to its tetrahedral base plate, PK2.1 has a predetermined breaking point in the contact area with the building platform. This prevents a serious deviation of the total weight due to a varying test specimen volume after separation from the building platform. On the square base plate with an edge length of 12 mm, supports are inserted which allow a connection to the final cover plate. Support structures with different parameter combinations are inserted in the area between the cover plate and the base plate. The cover plate thus simulates the component to be supported and the base plate the building platform. The area filled with support structures has a different removability of the residual powder depending on the used support structure parameters and is thus suitable for determining the material consumption considering different tooth geometries, perforations or

fragmentations. The test specimen can be built on different machines with a minimum build platform size of 250 x 250 mm in 81 parameter combinations to enable a low but meaningful and expandable test effort.

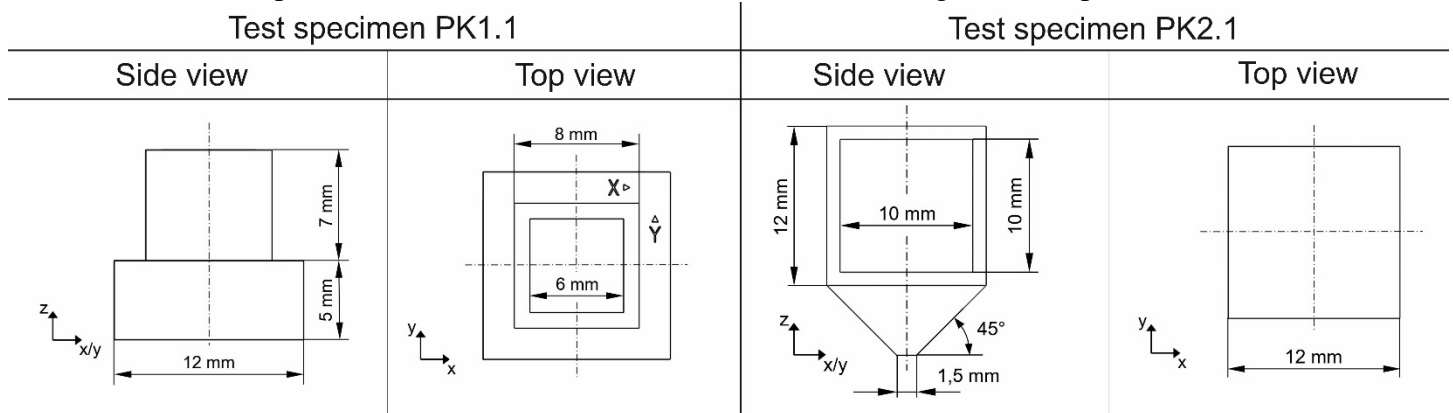| Test specimen PK1.1		Test specimen PK2.1	
Side view	Top view	Side view	Top view

Figure 3: PK1.1 specimen for investigating dimensional deviations, imaging accuracy and surface quality (left) and PK2.1 specimen for investigating material consumption.

The application-oriented test specimens (PK3.1 to PK3.7) described in the following are not investigated using all 81 parameter combinations. Based on the results of the pre-probing tests on PK1.1 and PK2.1, only the most promising support structure parameter combinations are used. So PK3.1 to PK3.7 allow an application-oriented validation of the most promising support structure parameter combinations with reduced experimental effort. To assess the suitability of the most promising support structures, various test specimens are developed, each representing a specific application situation. Standard elements are used, which have already been established in other scientific work [13, 15, 16]. For this purpose, non-curved, single-curved and double-curved standard elements with different attribute characteristics are investigated and the effect of support on these widely used geometric elements is investigated (PK3.1 to 3.5). In addition, removability under restricted accessibility is evaluated (PK3.7) and the change in the top length of the teeth as a function of the downskin angle of the supported surface is examined more in detail (PK3.6).

The PK3.1 test specimen shown in Figure 4 was developed to evaluate the support effect that can be achieved on externally supported, non-curved base elements. It consists of differently inclined overhangs in two different length and width steps. Non-curved overhangs are application-oriented geometries, which simulate downskin surfaces having the same normal vector at every point. Thus, the influence of the downskin angle on different quality criteria will be investigated.
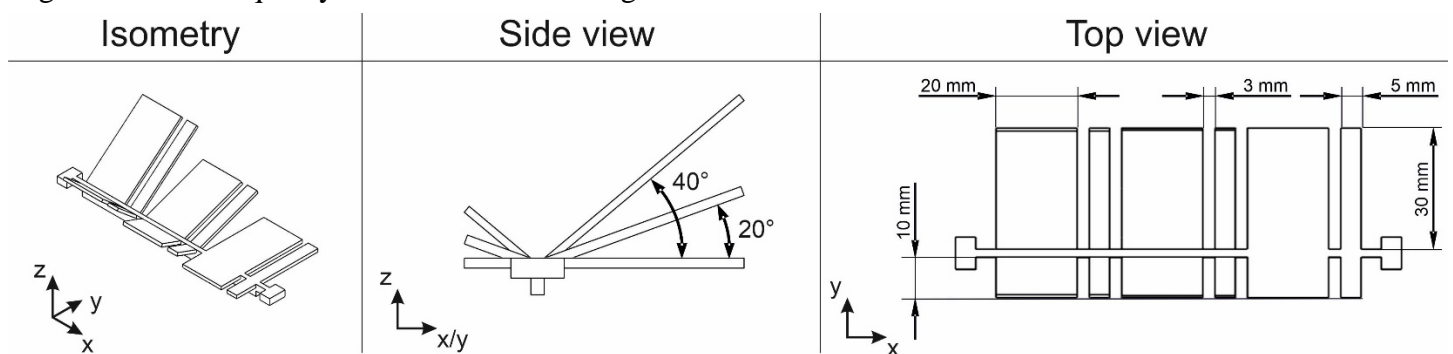
Isometry	Side view	Top view

Figure 4: Test specimen PK3.1 - external non-curved

The angle of the overhangs referring to the building platform is 0°, 20° and 40° and thus covers the range between a horizontal orientation of the downfacing surface of the component and the self-supporting angle, above which the use of solid support structures is unnecessary. Different literature values exist for this purpose. According to CALIGNANO, component surfaces must be supported below a relative angle of 30°, GRALOW ET AL. state a value of 40° and according to ADAM the limit value is 45°. For the following test specimens, an angle of 40° is chosen as the maximum value of the orientation [16, 20, 23]. In addition to the orientation of the overhangs, their width and length are varied. With increasing length, the path for dissipation

of thermal energy increases [16]. Increased negative influences of gravity and residual stresses can be detected at overhangs during the process [21]. With test specimen PK3.1, overhangs with a length of 10 mm and 30 mm projected onto the building platform are investigated. For the support of the overhangs, their width is also decisive. This is varied between 5 mm and 20 mm. The solid center bar ensures robust fabrication and subsequent clampability in the test fixture. After production, a measurement of the shape and dimensional accuracy is carried out on the build platform. The scientific investigations are carried out using the Nikon Altera® 8.7.6 coordinate measuring machine with the Renishaw® PH10M Plus rotary swivel head, the Renishaw® SP25M probe holder and the Renishaw® SP25_L40_D2 probe. After removing the support structures from the build platform, the measurement is repeated. In this way, any further distortion due to residual stress can be determined. In addition, a Keyence VR3200® macroscope is used to check the shape and dimensional accuracy of the cross-sectional profile of the overhanging beams and to examine the surface roughness of the downskin surfaces in accordance with DIN EN ISO 4288 and DIN EN ISO 3274 [16, 26].

Internal non-curved contours are also investigated in order to simulate application cases such as cavities or cooling channels [4]. For this reason, the influence of the support structures on differently inclined, internal, non-curved base elements is investigated on the test specimens PK3.2.1, PK3.2.2 and PK3.2.3 shown in Figure 5.
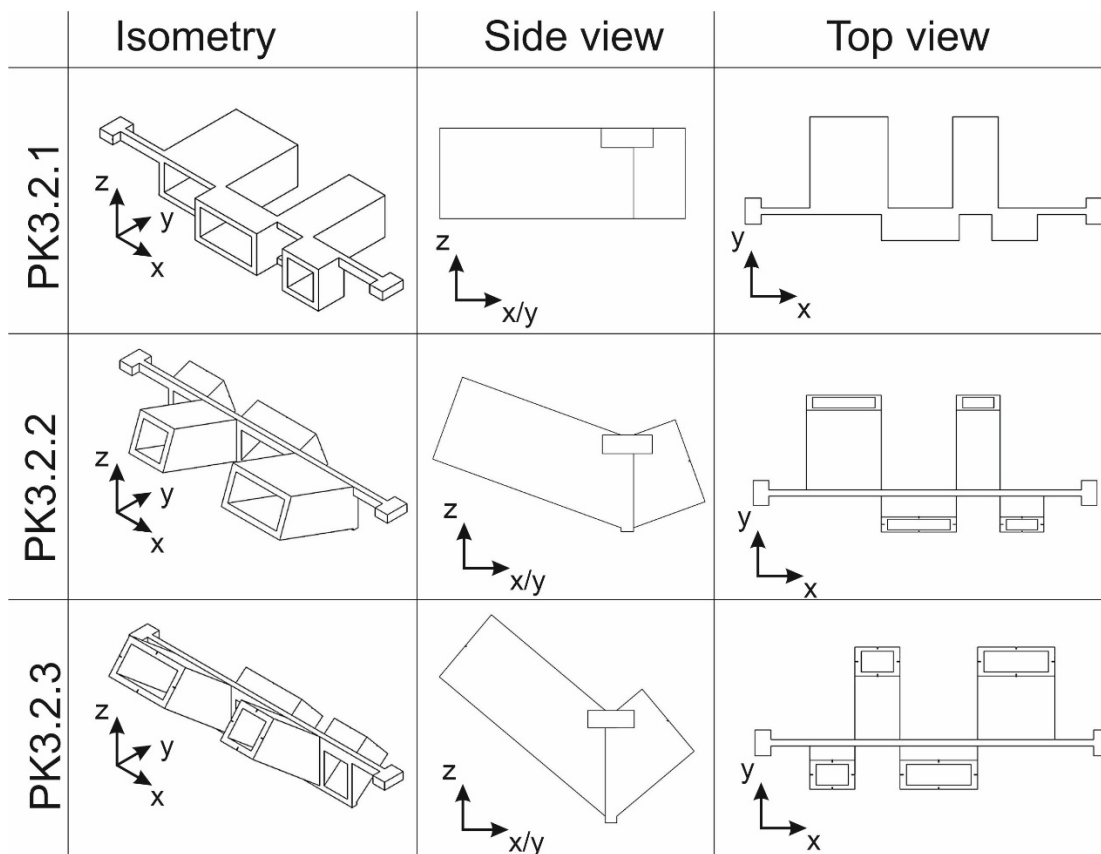

Figure 5: Test specimen PK3.2.1 with 0° orientation, PK3.2.2 with 20° orientation and PK3.2.3 with 40° orientation

The considered orientations correspond to 0°, 20° and 40° for the non-curved standard elements on external surfaces. The projected length of the surface to be supported is also identical at 10 mm and 30 mm, respectively. Spacings of 10 mm and 20 mm between the vertical walls were selected for the internal support structures. The wall thickness is 2 mm. The removability of the support structures from the internal, non-curved contours is investigated on the test specimens. After the support structure has been removed, a measurement of the cross-sectional profile is made and the surface roughness of the supported surfaces is examined.

In addition to the non-curved standard elements, many components also show single-curved standard elements in their geometry. Analogous to the test specimen PK3.1 for the examination of non-curved, external standard elements and PK3.2 for the examination of non-curved internal standard elements,

examinations of single-curved standard elements are carried out on the test specimens PK3.3 and PK3.4.1, PK3.4.2 and PK3.4.3. Here, the same quality criteria are examined using the same measuring techniques. The Specimens are shown in Figure 6.
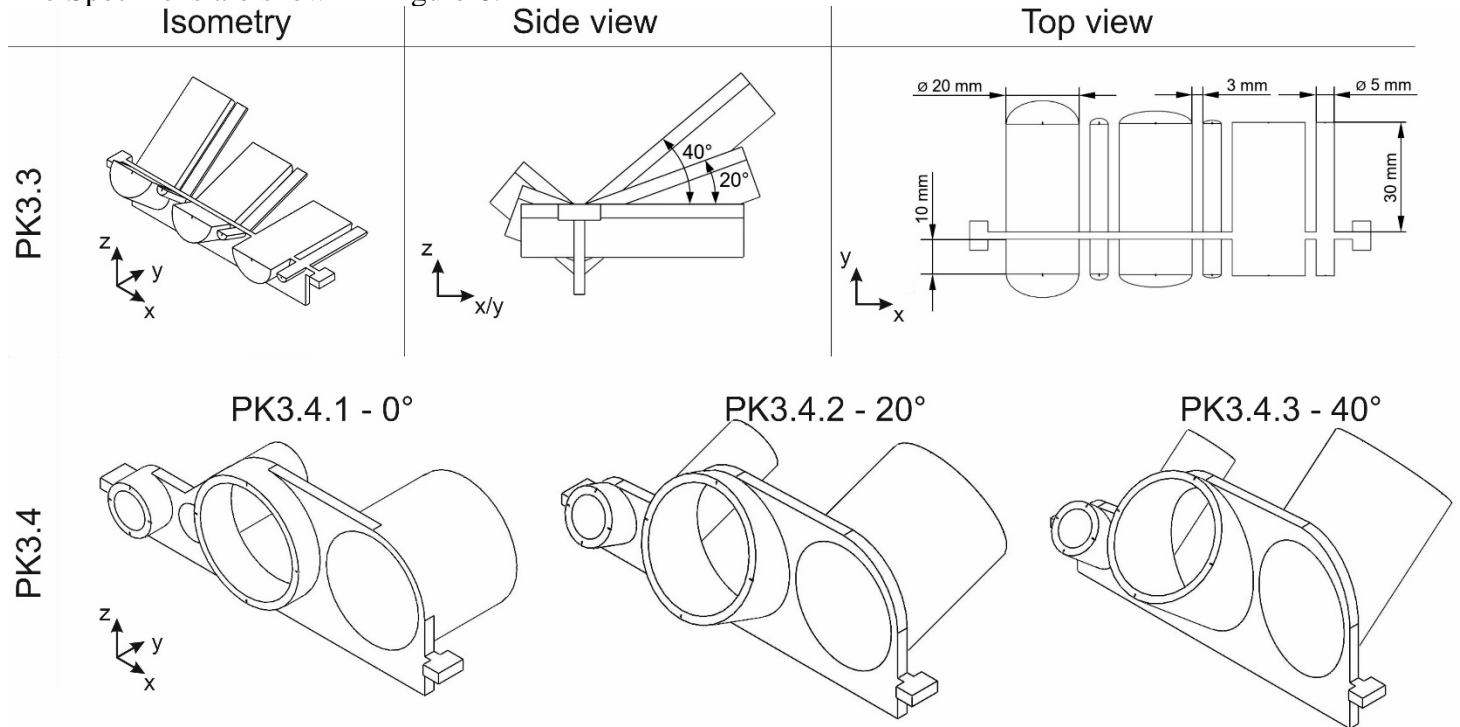

Figure 6: Test specimen PK3.3 - external single-curved (top) and test specimen PK3.4.1 to 3.4.3 - internal single-curved (bottom).

Other widely used standard elements are double-curved standard elements. The PK3.5 specimen shown in Figure 7 is used to investigate the support quality on convex and concave geometries. Both the inward-curved (concave) and outward-curved (convex) double-curved standard elements are examined with the three different diameter grades of 5 mm, 10 mm, and 20 mm. Height images are taken on the double-curved standard elements placed on specimen PK3.5 for the qualitative evaluation of the shape and dimensional accuracy as well as for the assessment of remaining support structure residues.
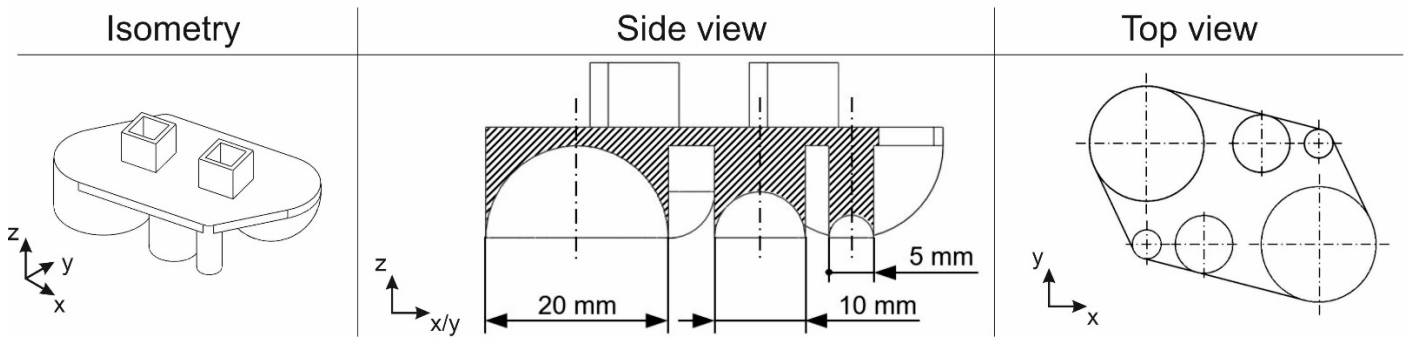

Figure 7: Test specimen PK3.5 – external and internal double curved.

The investigation of the test specimen PK3.6 shown in Figure 8 is an extension of the investigations on test specimen PK3.1. The contact situation between the component and the support structure is usually described by the component geometry. This changes the angle of intersection with the support structures and causes a change in tooth geometry. For this purpose, the PK3.6 specimen has a downskin surface with four subdivisions, which have a downskin angle of 10°, 20°, 30° and 40°. The width of the specimen is 5 mm. Here, after separation from the build platform, an optical examination of the top length for the different downskin angles can be carried out with the aid of a macroscope.

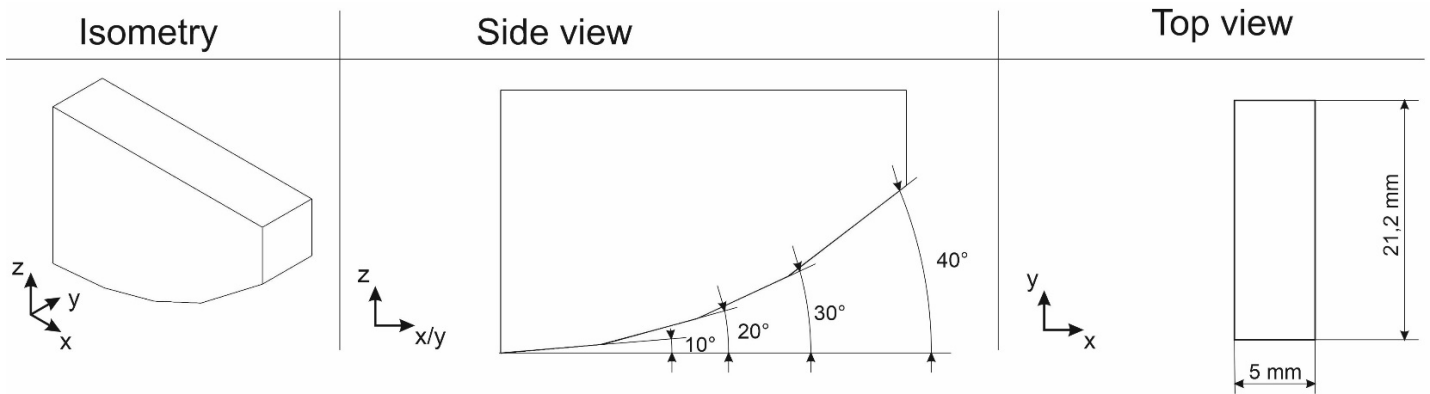| Isometry	Side view	Top view

Figure 8: Test specimen PK3.6 – downskin angle.

The PK3.7 specimen shown in Figure 9 is used to investigate the support removability with one-sided and two-sided accessibility. It is divided into two sections. On the left side, there is accessibility to the internal support structure on two sides, while on the right side the support is surrounded by solid walls on five sides. The test specimen is first removed from the building platform and then examined regarding removability. For this purpose, the time required to remove the support structure with a least possible residue is determined. As qualitative evaluation criteria, the necessary use of tools is determined, and the remaining support and powder residues are examined.
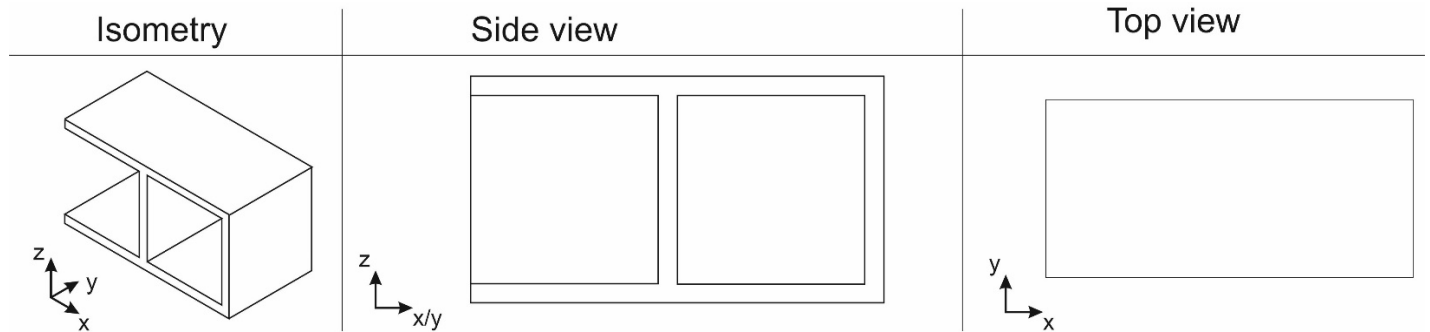
Isometry	Side view	Top view

Figure 9: Test specimen PK 3.7- support removability.

Step 3: Production of the test specimens under variation of the support

PK1.1 and PK1.2 are manufactured with 81 different parameter combinations of the support structures. A separate build job is provided for each of the test specimens PK1.1 and PK2.1. The positioning of the test specimens with the different parameter level combinations for build job 1 is shown in Figure 10 on the left. The orientation of the test specimens is parallel to the recoater lip. This orientation is indispensable for the subsequent metrological examination on a coordinate measuring machine and is justifiable in terms of production technology due to the small component dimensions. In addition, the orientation ensures maximum loading of the test specimens by the recoater, thus putting the durability of the support structures against process forces to the test [4]. The distance between the test specimens is 10 mm to facilitate measurement and detachment and to avoid mutual interferences between the support structures and test specimens due to the arrangement. The build jobs can be manufactured on machines with a build platform size of 250 x 250 mm or larger. A reference block is inserted for measurement by means of a coordinate measuring machine. The build jobs are produced in multiple realizations, considering randomization and block formation to eliminate global changes in boundary conditions during production, such as ambient temperature or powder charge, as well as local thermal differences across the build platform from the results. Figure 10 on the right shows the position names on the build platform. Between several realizations, the assignment of the different parameter level combinations to the position names has to be randomized. The fabrication was carried out on a SLM Solutions SLM 250HL system using the material 316L (1.4404) and the parameter set 316L_SLM_MBP3.0_ 50_CE2_400W_Stripes_V2.0.
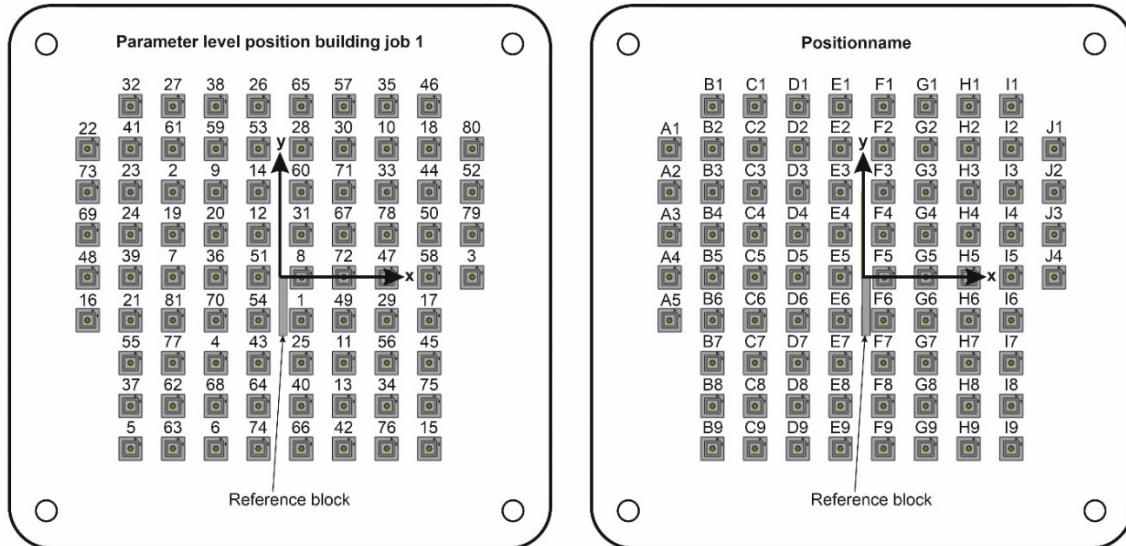
Figure 10: Realized arrangement of the test specimens parameter for build job 1(left) and general positionames (right).

PK3.1 to PK3.6 are also manufactured under the described boundary conditions. However, not all 81 paremeter combinations of the support structures are considered here. This would increase the test effort and the costs of the test specimen production too much. Instead, the best parameter combination from the pre-probing at PK1.1 and PK2.1 are selected and used to support PK3.1 to 3.7. In this context, PK3 represents test specimen geometries close to the application, which allow validation of the results from the pre-probing and were developed based on established standard elements [16]. The arrangement of PK 3.1 to PK3.7 is shown in Figure 11. In addition, a problem-specific adaptation of the build job can be performed by removing test specimens not related to the application to reduce the experimental effort. Further on, an area for freely selectable test specimens is provided. This allows to place test specimens for the calibration and verification of a numerical simulation or tensile tests.
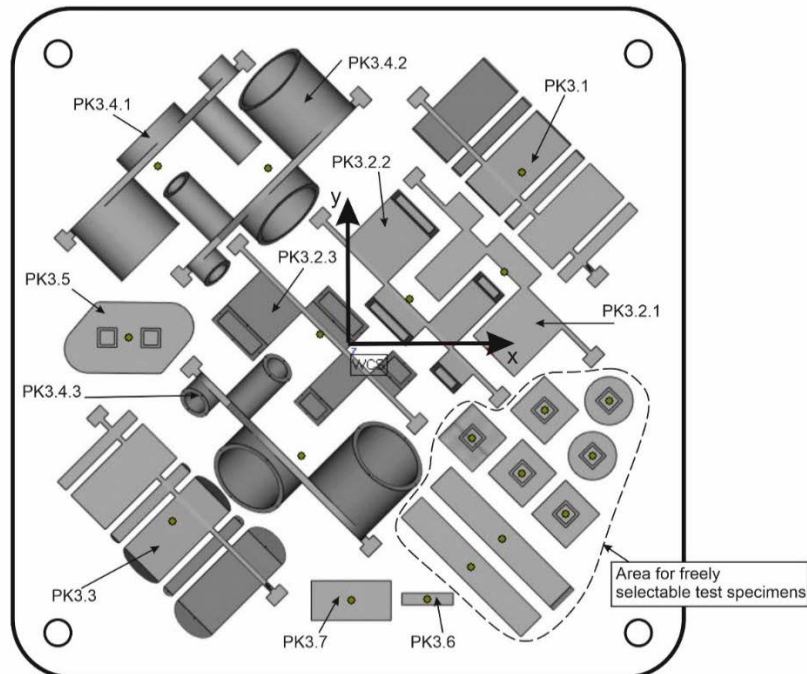

Figure 11: Arrangement of the test specimens PK3.

Step 4: Examination and evaluation of the test specimens with regard to the quality criteria

As an example, the examination of shape and dimensional accuracy in the xy -plane is listed below and the graphical evaluation is described. The investigations for the other quality criteria were evaluated analogously, so that diagrams as shown in Figure 12 exist for each quality criterion.
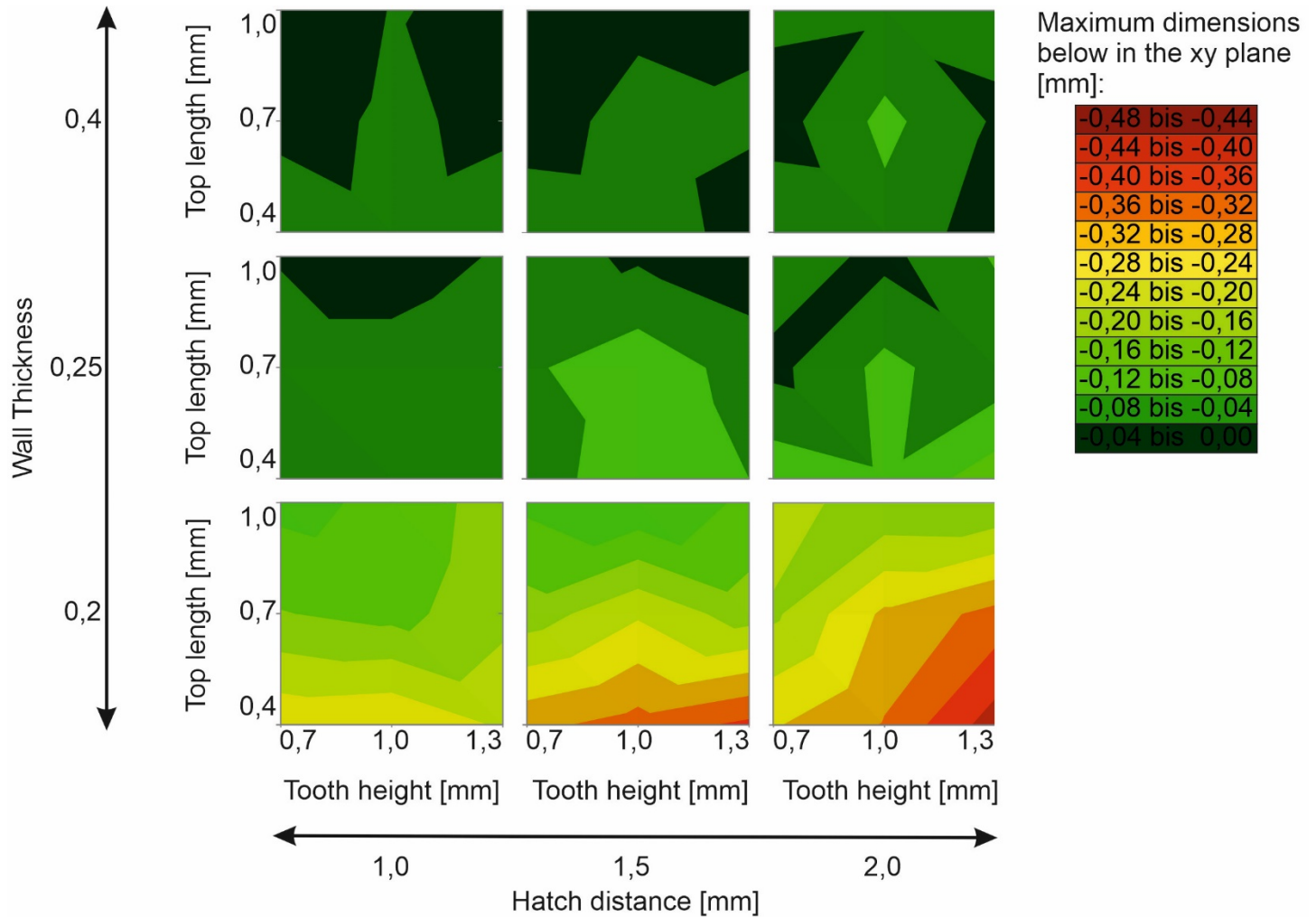

Figure 12: Overall result plot of shape and dimensional accuracy in the xy plane (maximum dimension below deviation).

To investigate the shape and dimensional deviation in the xy plane, eight measuring points were probed on the PK1.1 specimen with the Nikon Altera® 8.7.6 coordinate measuring machine, two on each of the four side faces with an offset of 1 mm in the z direction from the top and bottom edges of the specimen. For evaluation, the maximum dimensions below the nominal dimension was calculated. Figure 12 shows the maximum dimension below for all investigated parameter level combinations. Here, the abscissa shows the hatch distance of the support structures in three parameter levels and the ordinate shows the wall thickness of the support structures. Each smaller, colored square in the coordinate system represents a separate additional diagram in which the tooth geometry was varied on the basis of tooth height and top length. In this overall result display, all possible combinations of hatch distance, wall thickness, top length and tooth height can be quickly compared with each other. The quality criterion maximum dimension below deviation in the xy-direction is quantified by the color scheme. The dark green areas thus represent parameter level combinations that exhibit a particularly low dimensional deviation. Reddish shades represent a greater dimensional deviation. Detailed values can be found in the legend.

The overall result plot in Figure 12 shows a clear correlation between the wall thickness parameter and the maximum dimension below of the specimen width in the xy plane. Whereas with a wall thickness of 0.25

234

mm or 0.4 mm the dimension below does not exceed a value of -0.160 mm, a wall thickness of 0.2 mm (depending on the choice of the other parameters) shows a deviation of up to -0.424 mm. This variant of the block support at this location has a hatching of 2 mm, a top length of 0.4 mm and a tooth height of 0.7 mm. Overall, there is an increased dimension below with reduction in wall thickness. This can be explained by a decrease in deformation resistance, which cannot prevent contraction of the solidifying and cooling material.

When comparing the measurement results in the bottom row of the overall results plot, an increase in the dimension below with an increase in the size of the hatching also becomes apparent. This can be seen in the comparison of the three support variants, which have a wall thickness of 0.2 mm, a top length of 0.4 mm and a tooth height of 1.3 mm. No comparable influence can be seen with a wall thickness of 0.25 mm or 0.4 mm. Obviously, the deformation resistance of the single support wall at corresponding wall thicknesses is sufficient to compensate the lower number of support walls when the hatch distance is increased. Based on the bottom row, the influence of the top length can also be observed. It can be clearly seen that with an increase in the contact length of the teeth to the supported surface, a reduction in the maximum dimension below can be achieved. This effect can also be attributed to an increase in deformation resistance due to the larger total contact area. No comparably clear correlation is shown for the tooth height. While an increase in the dimension below with an increase in the tooth height can be observed for a wall thickness of 0.2 mm and a hatching of 2 mm (right field of the bottom row), this influence cannot be seen for a center distance of 1 mm or 1.5 mm. With a greater wall thickness of 0.25 mm or 0.4 mm, there is also no influence of this parameter. An increase in tooth height appears to have a negative effect only with a simultaneous weakening of the support structure due to a reduced wall thickness and an increased hatch distance. The effects and interactions of the individual support structure parameters on the quality criterion can be seen in the effect diagram in Figure 13.
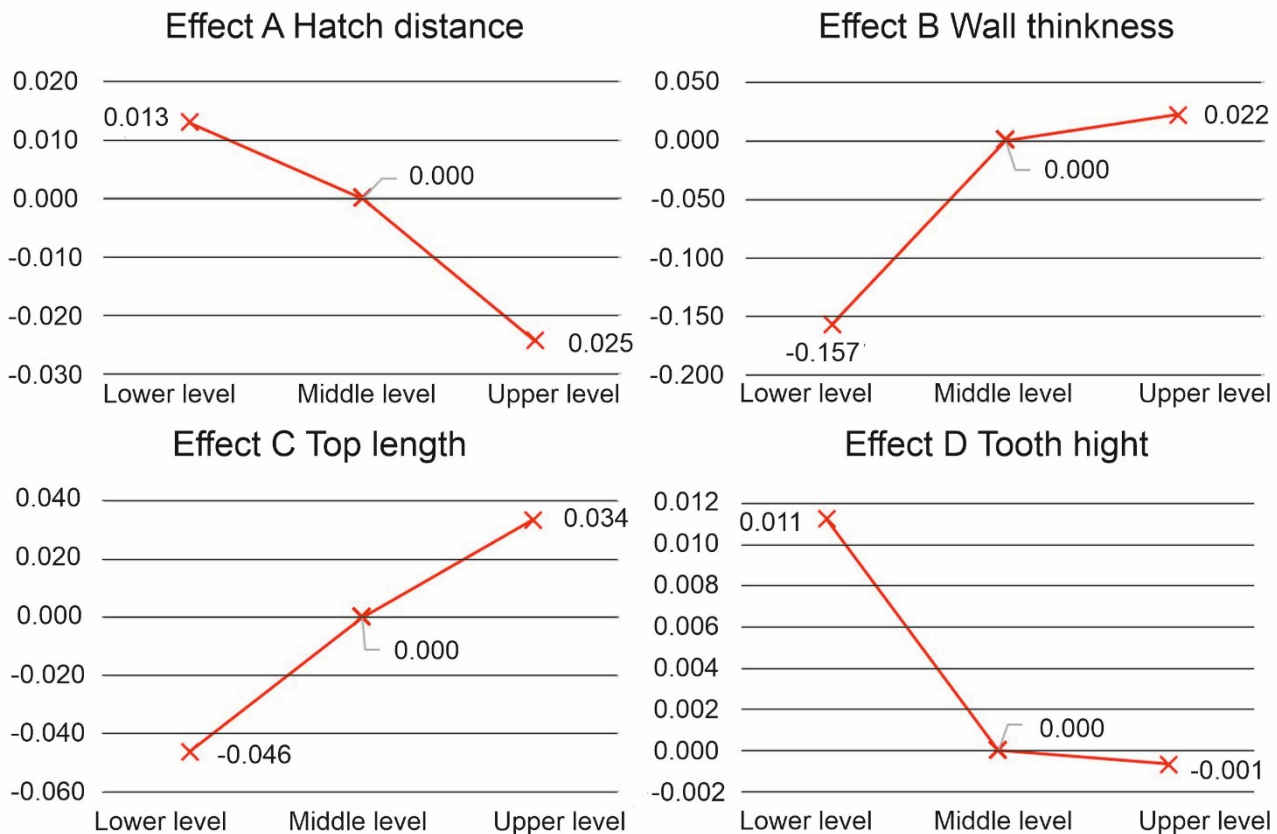

Figure 13: Effect diagram for different parameters for dimensional accuracy in the xy plane (maximum dimension below deviation).
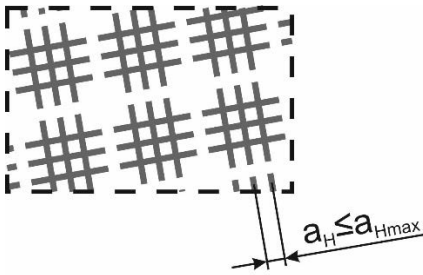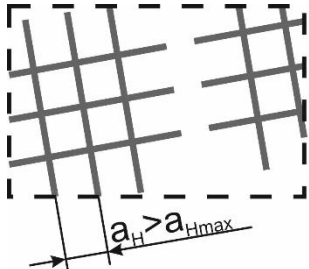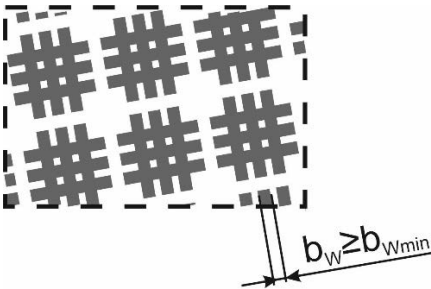
A comparison of the four investigated support structure parameters shows that wall thickness (B) has most significant influence on the quality criterion dimensional accuracy in the xy-plane. If the wall thickness is reduced from the medium level of 0.25 mm to the minimum possible value of 0.2 mm, the maximum dimensional deviation increases by -0.157 mm on average. If, in the opposite direction, the parameter is

increased to a value of 0.4 mm, there is a decrease in the dimensional undershoot of 0.022 mm. The influence of the hatching (A) and the tooth height (D) is comparatively small in the considered value ranges of the parameters with 0.038 mm and 0.012 mm, respectively. In both cases, an increase in the dimension below can be observed when the parameter is increased. The top length (C) of the teeth shows a more significant influence. Increasing this parameter from 0.4 mm initially to 1 mm reduces the dimension below in the xy plane by 0.080 mm on average. However, comparing all parameters, increasing the wall thickness can be recommended as the most effective measure to reduce the dimension below. The dominance of effect B by adjusting the wall thickness can also be seen from the 2-factor interactions. The course of the 2-factor interaction AB, BC and BD corresponds approximately to that of effect B.

Step 5: Derivation of design guidelines

Design guidelines can be derived on the basis of the results determined in step 4. In the following the design guidelines for the quality criterion of dimensional accuracy in the xy-plane are exemplarily presented in Table 1. Design guidelines for other quality criteria were derived analogously. For this purpose, the results of the effect calculations for the individual support structure parameters are summarized in written form and visualized with the aid of a drawing "suitable for production" and one "not suitable for production". To determine the listed limit values a_{Hmax}, b_{Wmin}, l_{Tmin} and h_{Zmax}, use the overall result representation in Figure 12. It should be noted that the limit values are dependent on the other three parameters and therefore no globally valid values can be given. The limit values are therefore dependent on the selected support structures and on the boundary conditions such as machine, material and production parameters.

Table 1: Design guidelines for production-suitable support structures with regard to the quality criteria shape and dimensional accuracy in the xy plane (maximum dimension below deviation).
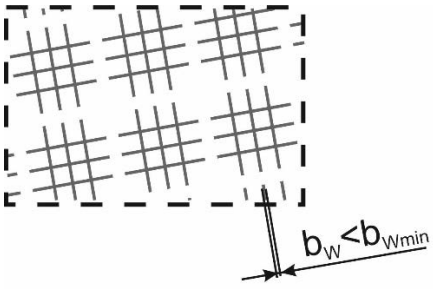
Hatch distance of support structures (Effect A)		
Description: The hatch distance a_H of adjacent retaining walls should be chosen as small as possible to minimize the dimension below in the xy-plane.	Suitable design $a_H \leq a_{Hmax}$	Unsuitable design $a_H > a_{Hmax}$
Wall thinkness of support structures (Effect B)		
Description: The wall thickness b_W of support walls should be chosen as large as possible to minimize the dimension below in the xy-plane.	Suitable design $b_W \geq b_{Wmin}$	Unsuitable design $b_W < b_{Wmin}$

Top length of support teeth (Effect C)		
Description: The top length l_T of the support teeth should be chosen as large as possible to minimize the dimension below in the xy plane	Suitable design $l_T \geq l_{Tmin}$	Unsuitable design $l_T < l_{Tmin}$

Height of support teeth (Effect D)		
Description: The height h_Z of the support teeth should be chosen as low as possible to minimize the dimension below in the xy plane	Suitable design $h_Z \leq h_{Zmax}$	Unsuitable design $h_Z > h_{Zmax}$

Additional influences through effect interactions
The wall thickness (parameter effect B) dominates over the other parameter effects →The increase of the wall thickness represents the most efficient measure to reduce the dimensional undershoot in the xy-plane

Conclusion and outlook

One of the hurdles to more widespread industrial use of the LPBF process is the unavoidable use of solid support structures. Their utilization, caused by a variety of tasks they fulfil, affects part quality and process efficiency. To counteract the disadvantages and to gain a comprehensive process understanding with regard to support structures, this publication deals with the development of a method to derive production-oriented design guidelines for support structures. Based on application-relevant quality criteria such as shape- and dimensional accuracy, surface roughness, removability, data preparation time, data volume and material consumption, test specimens were developed and manufactured. To examine the test specimens, a standardized procedure was developed to show the influence of various support structure parameters on the quality criteria. As a result, the designer receives a graphical representation of the influence that each parameter has onto the quality criteria. This graphical representation can be used as a well-founded basis for the selection of an application-specific suitable support structure as well as for the deriving of design guidelines.

To extend the results, it is possible to investigate further support structures or to vary further boundary conditions such as the manufacturing equipment, the material or the manufacturing parameters. Due to the modular structure of the method, this is feasible in an easy way. For example, the procedure can be used to build up a database for support structures. The integration and evaluation of the results in a neural network for the prediction of the influence of further support structure parameters on the quality criteria also seems to be auspiciously.

Literature

[1] GEBHARDT, A.: Generative Fertigungsverfahren – Additive Manufacturing und 3D Drucken für Prototyping - Tooling - Produktion. 4. Auflage, Carl Hanser Verlag, München, ISBN 978-3-446-43651-0, 2013

[2] BERGER, U.; HARTMANN, A.; SCHMID, D.: 3D-Druck - Additive Fertigungsverfahren – Rapid Prototyping, Rapid Tooling, Rapid Manufacturing. 2. Auflage, Verlag Europa-Lehrmittel - Nourney Vollmer GmbH & Co. KG, Haan-Gruiten, ISBN 978-3-8085-5034-2, 2017

[3] FELDMANN, C.; PUMPE, A.: 3D-Druck - Verfahrensauswahl und Wirtschaftlichkeit – Entscheidungsunterstützung für Unternehmen. Springer Gabler, Wiesbaden, 2016 - ISBN 978-3-658-15195-9

[4] KRANZ, J.; HERZOG, D.; EMMELMANN, C.: Design guidelines for laser additive manufacturing of lightweight structures in TiAl6V4. In: Journal of Laser Applications, Vol 27 S14001, 2015.

[5] CAVIEZEL, C.; GRÜNWALD, R.; EHRENBERG-SILIES, S.; KIND, S.; JETZKE, T.; BOVENSCHULTE, M.: Additive Fertigungsverfahren (3-D-Druck) – Innovationsanalyse. Büro für Technikfolgen-Abschätzung beim Deutschen Bundestag, Berlin, 2017. Unter: https://www.tab-beim-bundestag.de/de/pdf/publikationen/berichte/TAB-Arbeitsbericht-ab175.pdf, zuletzt geprüft am 13. März 2019

[6] WESSARGES, Y.; GIESEKE, M.; HAGEMANN, R.; KAIERLE, S.; OVERMEYER, L.: "Entwicklungstrends zum Einsatz des selektiven Laserstrahlschmelzens in Industrie und Biomedizintechnik." In: Lachmayer, R.; Lippert, R. B. (Hrsg.): Additive Manufacturing Quantifiziert – Visionäre Anwendungen und Stand der Technik, Springer Verlag GmbH, Berlin, Heidelberg, 2017 - ISBN 978-3-662-54112-8

[7] MORGAN, D.; AGBA, E.; HILL, C.: Support Structure Development and Initial Results for Metal Powder Bed Fusion Additive Manufacturing. In: Procedia Manufacturing, 45th SME North America Manufacturing Research Conference. Vol. 10, 2017, Elsevier B.V., Amsterdam, S. 819-830. DOI: 10.1016/j.promfg.2017.07.083

[8] MILEWSKI, J. O.: Additive Manufacturing of Metals – From Fundamental Technology to Rocket Nozzles, Medical Implants and Custom Jewelry. Springer Series in Material Science, Band 258, Springer International Publishing, Cham, 2017 - ISBN 978-3-319-58204-7

[9] VEREIN DEUTSCHER INGENIEURE: VDI 3405 Blatt 3: Additive Fertigungsverfahren –Konstruktionsempfehlungen für die Bauteilfertigung mit Laser-Sintern und Laser-Strahlschmelzen. Beuth Verlag, Berlin, 2015.

[10] ASTM52900: „Additive manufacturing – General principles – Terminology", (ISO/ASTM DIS 52900:2018), Beuth Verlag, 2018

[11] GIBSON, I.; ROSEN, D.; STUCKER, B.: Additive Manufacturing Technologies – 3D Printing, Rapid Prototyping and Direct Digital Manufacturing. 2. Auflage, Springer Science+Business Media, New York, 2015 - ISBN 978-1-4939-2112-6

[12] LAMMERS, S.; TOMINSKI, J.; MAGERKOHL, S.; KÜNNEKE, T.; LIENEKE, T.; ZIMMER, D.:"Design Guidelines for a Software-Supported Adaptation of Additively Manufactured Components with Regard to a Robust Production" 29th Annual International Solid Freeform Fabrication (SFF) Symposium – An Additive Manufacturing Conference. Texas, Austin, USA, 13.08.2018 - 15.08.2018. University of Texas, S. 527-540, 2018

[13] LAMMERS, S.; TOMINSKI, J.; ZIMMER, D.: „Guidelines for post processing oriented design of additive manufactured parts for use in topology optimization" In: Auricchio, Ferdinando; Rank, Ernst.; Kollmannsberger, Stefan.; Morganti, Simone: Proceedings of II. International Conference on Simulation for Additive Manufacturing Sim-AM 2019, Pavia, Italy, September 11-13, 2019, S. 174-185; ISBN: 978-84-949194-8-0, 2019

[14] KÜNNEKE, T.; LIENEKE, T.; LAMMERS, S.; ZIMMER, D.: „Design guidelines for post-processing of laser beam melting in context of support structures" In: Bernard, Alain; Leach, Richard; Pedersen, David Bue; Taylor, John: Proceedings of the Special Interest Group meeting on Advancing Precision in Additive Manufacturing, Ecole Centrale de Nantes, France; S. 137-140; ISBN: 978-0-9957751-5-2, 2019

[15] Forschungsberichte des Direct Manufacturing Research Centers; Herausgeber: PROF. DR.-ING. IRIS GRÄßLER, UNIV.-PROF. DR.-ING. RAINER KOCH, PROF. DR.-ING. HABIL. HANS ALBERT RICHARD, PROF. DR. HANS-JOACHIM SCHMID, PROF. DR.-ING. VOLKER SCHÖPPNER, PROF. DR. RER. NAT. THOMAS TRÖSTER, PROF. DR.-ING. DETMAR ZIMMER, PROF. DR.-ING. HABIL. MIRKO SCHAPER UND PROF. DR.-ING. ELMAR MORITZER; Band 25: Rainer Koch, Iris Gräßler, Detmar Zimmer, Thomas Tröster (Hrsg.): „Mehrzieloptimierte und durchgängig automatisierte Bauteilentwicklung für Additive Fertigungsverfahren im Produktentstehungsprozess - Ergebnisbericht des BMBF Verbundprojektes OptiAMix"; ISBN:978-3-8440-7932-6; Paderborn, 04. 2021

[16]   ADAM, G. A. O.: Systematische Erarbeitung von Konstruktionsregeln für die additive Fertigungsverfahren Lasersintern, Laserschmelzen und Fused Deposition Modeling. PhD-Thesis, Paderborn University, Shaker, Aachen, 2015.

[17]   THOMAS, D.: The Development of Design Rules for Selective Laser Melting. PhDThesis, University of Wales Institute, 2009.

[18]   TOMINSKI, J.; LAMMERS, S.; WULF, C.; ZIMMER, D.: "Method for a Software-Based Design Check of Additively Manufactured Components" 29th Annual International Solid Freeform Fabrication (SFF) Symposium – An Additive Manufacturing Conference. Texas, Austin, USA, 13.08.2018 - 15.08.2018. University of Texas, S. 69-79, 2018

[19]   LANGELAAR, M.: „Integrated component-support topology optimization for additive manufacturing with post machining", Rapid Prototyping Journal Vlume 25 Issu 2, Emerald Insight, ISSN: 1355-2546, 2019

[20]   GRAWLOW, M.; BLUNK, H.; IMGRUND, P.; HERZOG, D.; EMMELMANN, C.: Design Guidelines zur Auswahl geeigneter Supporttypen für verschiedene Anwendungsfälle im Bereich Laserstrahlschmelzen – Auf dem Weg zur automatisierten Supportgenerierung. In: Rapid.Tech - Fachkongress, Forum Konstruktion. Carl Hanser Fachbuchverlag, München, 2018, S. 95-110

[21]   JÄRVINEN, J.-P.; MATILAINEN, V.; LI, X.; PIILI, H.; SALMINEN, A.; MÄKELÄ, I.; NYRHILÄ, O.: Characterization of effect of support structures in laser additive manufacturing of stainless steel. In: Physics Procedia, 8th International Conference on Photonic Technologies. Vol. 56, 2014, Elsevier B.V., Amsterdam, S. 72-81. DOI: 10.1016/j.phpro.2014.08.099

[22]   KLAHN, C. (HRSG.); MEBOLDT, M. (HRSG.); FONTANA, F.; LEUTENECKER-TWELSIEK, B.; JANSEN, J.: Entwicklung und Konstruktion für die Additive Fertigung – Grundlagen und Methoden für den Einsatz in industriellen Endkundenprodukten. Vogel Business Media GmbH & Co. KG, Würzburg, 2018 - ISBN 978-3-8343-3395-7

[23]   CALIGNANO, F.: Design optimization of supports for overhanging structures in aluminum and titanium alloys by selective laser melting. In: Materials & Design. Vol. 64, 2014, Elsevier Ltd., London, S. 203-213. DOI: 10.1016/j.matdes.2014.07.043

[24]   GAN, M. X.; WONG, C. H.: Practical support structures for selective laser melting. In: Journal of Materials Processing Technology. Vol. 238, 2016, Elsevier B.V., Amsterdam, S. 474-484. DOI: 10.1016/j.jmatprotec.2016.08.006

[25]   DIN EN ISO 4288: Geometrische Produktspezifikation (GPS) – Oberflächenbeschaffenheit: Tastschnittverfahren - Regeln und Verfahren für die Beurteilung der Oberflächenbeschaffenheit, 1998

[26]   DIN EN ISO 3274: Geometrische Produktspezifikation (GPS) – Oberflächenbeschaffenheit: Tastschnittverfahren - Nenneigenschaften von Tastschnittgeräten, 1998